

Ship Damage Stability Enhancement through Crashworthiness

Hongseok Bae, *Sharjah Maritime Academ, Khorfakkan, Sharjah, UAE*, hongseok.bae@sma.ac.ae

Dracos Vassalos, *Sharjah Maritime Academy , Khorfakkan, Sharjah, UAE*, dvassalos@sma.ac.ae

Donald Paterson, *Sharjah Maritime Academy, Khorfakkan, Sharjah, UAE*, donald.paterson@sma.ac.ae

Francesco Mauro, *Sharjah Maritime Academy , Khorfakkan, Sharjah, UAE*, Francesco.Mauro@sma.ac.ae

ABSTRACT

Crashworthiness as one of the Risk Control Options (RCOs) for damage stability enhancement has been around since the 1990s, potentially earlier. Yet, it has never managed to gain inroads for routine use in ship design and operation to enhance ship damage stability cost-effectively, more specifically targeting passenger ships. A key reason relates to lack of understanding of how the concept can be used in ship design or design upgrades to enhance damage stability, especially since this requires a complete risk assessment of this RCO adopting the Alternative Design and Arrangements methodology, which could be time-consuming and only possible through expert guidance. The latter is also linked to lack of efficient tools to undertake such analysis routinely as well as a lack of in-depth research and experiential knowledge on how best to benefit from this concept. This paper attempts to cover these gaps and provide proof of concept evidence by considering damage stability upgrade of a cruise ship through crashworthiness. Other risk control options are also evaluated, for comparative assessment of cost-effectiveness, leading to useful conclusions and guidelines on how to use the crashworthiness concept as a credible risk control option for damage stability enhancement.

Keywords: *Crashworthiness, Damage stability, Flooding Risk Assessment, RCOs, Ship Collision*

1 INTRODUCTION

After the Titanic accident, SOLAS regulations were established and strengthened to enhance ship safety pertaining to flooding risk. SOLAS 1948 introduced deterministic methods for ship stability criteria, and SOLAS 2009 probabilistic methods with additional deterministic criteria based on the righting levers (GZ-curve) of the ship, residual metacentric height (GM), heeling angle range, heeling angle-righting arm area, and maximum righting arm (GZ). In particular, in SOLAS 2009, a new concept of damage stability assessment was introduced, which uses a probabilistic approach based on flooding occurrence probabilities for each longitudinal, transverse, side of damage, and vertical direction for each compartment zone. Both types of damage stability criteria have been widely applied to commercial vessels and passenger ships under different requirements in addition to SOLAS, such as MARPOL, ICLL, SPS code, Stockholm Agreement, etc.

Although the current SOLAS damage stability criteria have been effective in maintaining high standards of ship survivability against flooding accidents, many issues of concern are still embedded in these. The criteria assume that flooding occurs in all zones, which means that innovative structural designs, such as new structural arrangements and crashworthy material applications, are treated the same as a typical structure. Additionally, predetermined breach distributions (p-factors) lead to biased damage stability solutions that focus solely on ship survival improvement (s-factor), disregarding individual operating characteristics such as operating area and profiles.

To address crashworthy structure applications to ships, Germanischer Lloyd (IMO, 2003, Zhang et al., 2004) introduced a direct analysis as an approval procedure for alternative double-hull structure arrangements within the scope of the EU-funded project Crash Coaster, being suggested for adoption in the context of explanatory notes as contained in IMO Resolution A.684(17) (IMO, 1991). Unfortunately, this approval procedure has not been

successfully adopted as an IMO Resolution. Additionally, it only focused on physical crashworthiness analysis for ship-ship collision regarding collision energy and penetration using FE and no knowledge was introduced pertaining to ship damage stability for overall ship survivability.

This paper focuses on how to enhance overall ship survivability, pertaining to p-factors, with the application of crashworthy structural designs as risk control options (RCOs). As a direct assessment, crashworthiness analysis is employed to identify actual damage extents. Section 2 suggests a quantitative risk assessment methodology that provides equivalent damage stability criteria to the current SOLAS regulations within the IMO framework in a cost-effective way. Section 3 describes a practical demonstration using a reference vessel as a case study, including vulnerable zone identification, application of RCOs, FE analysis, and cost-benefit analysis. Six crashworthy RCOs as passive measures were investigated and the optimum RCO was selected for the final decision-making of related stakeholders.

2 QUANTITATIVE RISK ASSESSMENT METHODOLOGY

This proposed methodology places focus on improving damage stability using crashworthiness analysis to enhance survivability. Through structural crashworthiness analysis from the FE method, it is possible to estimate the reduction in damage extents from the application of crashworthy structural design alternatives (Risk Control Options), as illustrated in Figure 1. This leads to updated damage breach distributions and an impact on ship survivability. The cost-effectiveness of these Risk Control Options can be analysed using the Gross Cost of Averting a Fatality (GCAF) for ship survivability enhancement, taking into account both cost and risk reduction.

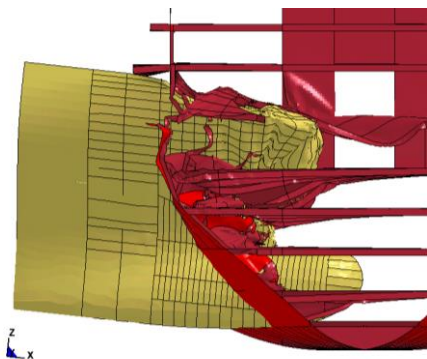


Figure 1 : Typical Crashworthiness Analysis on ship collisions

As a quantitative risk assessment, the proposed methodology consists of seven steps as follows;

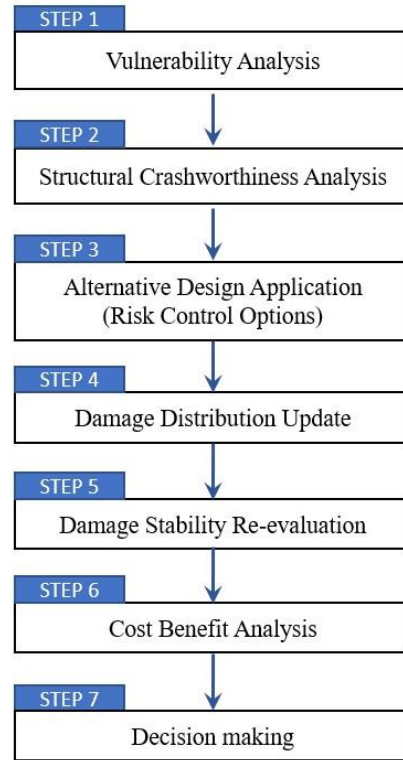


Figure 2 : Overall Methodology

Step 1: Vulnerability Analysis

The first step is to calculate the damage stability of the target ship using standard damage stability analysis according to current SOLAS 2020 regulations. Based on the calculation results, Equation (1) can be used to calculate the local Attained Index loss for the classification of high-risk zones. This enables the identification of the most vulnerable zone in the target ship.

$$Index\ Loss = \sum p_i \times (1 - s_i) \quad (1)$$

Next, one or two high-risk zones can be selected for RCO application to improve overall ship risk. To achieve this, the permeability of each subdivision zone can be manually set to zero (i.e., no flooding condition) to determine how much the Index can be improved. However, this manual calculation for all relevant compartments requires additional effort and increased calculation time. To address these problems, this paper proposes a vulnerability

analysis method, suggesting a plurality approach with extension to adjacent zones.

Step 2: Structural Crashworthiness Analysis

The next step involves conducting ship collision simulations for the target vulnerable zone. Since the structural response in ship collisions involves crushing, buckling, plasticity, and rupture, which are highly nonlinear, this paper adopts the nonlinear finite element method (NLFEM). This method is also recommended in ADN 2009 for alternative structure procedures (UN, 2008). Unlike the FE analysis method in ADN 2009, which employs restraint in three transitional freedoms, the proposed methodology takes into account actual ship motions with surrounding water effects using MCOL solver, such as added mass effects, restoring and wave damping forces. This enables the reflection of actual external dynamics between the two ships and coupling dynamics with internal collision mechanics.

Collision Scenario Definition

The selection of collision scenarios is a crucial factor in crashworthiness analysis for ship collisions since it directly affects the damage breach size results. Typically, six aspects are taken into account for collision scenarios, including striking ship, collision location, collision speed, collision angle, draught, and trim. This paper proposes a reasonable worst-case scenario within the current SOLAS framework. However, the final collision scenario should be discussed and approved by the relevant Administration based on the target ship's operating areas and profiles.

Striking ship: The striking ship is primarily related to the initial kinetic energy, which is determined by its mass and speed. Additionally, the bow shape directly affects the damage breach results. Therefore, it is reasonable to select the actual target striking vessel instead of using generalised bow shapes and assumptions. This paper recommends selecting a ship with a high probability of encountering a target ship based on its actual operational profile history, such as the IAS data of the target vessel.

Collision Speed: the primary determinant of the initial kinetic energy during a collision is the

collision speed of the striking vessel, which in turn significantly impacts the outcome of breach penetration. Numerous researchers have employed different collision speeds in their collision assessments. For instance, velocities ranging from 0.5 to 14 knots were used for a 179m Ropax ship (Schreuder et al., 2011), for a VLCC (Paik et al., 2017), for a 9,000 TEU container ship (Kim et al., 2021), for an Aframax (Zheng et al., 2007), and even as high as 19.44 knots (equivalent to 10 m/s) for a 310 LNG carrier (Ehlers et al., 2008). It is worth noting, however, that the kinetic energy at 19.44 knots is 15 times greater than that at 5 knots, leading to vastly distinct simulation outcomes. Therefore, in contrast to the previously used fixed collision speeds derived from accident databases, this paper introduces the concept of a "relative collision speed." This concept is defined as the specific speed that yields a B/2 penetration of the ship, as per the current SOLAS framework. This approach offers two main advantages. Firstly, the collision scenario aligns with the IMO framework, ensuring a collision case that is neither overly gentle nor excessively severe, adhering to the principle of regulation criteria of maximum penetration at B/2. Secondly, this concept could mitigate or harmonise discrepancies in damage extents resulting from uncertainties in simulation setups, encompassing variations in failure criteria and material behaviour. Consequently, the collision speed utilised in each analysis is adaptable to different collision scenarios and the crashworthiness analysis techniques employed by individual researchers. To determine the "relative collision speed" for achieving B/2 penetration, a series of preliminary simulations involving varying collision speeds were undertaken, as depicted in Figure 3.

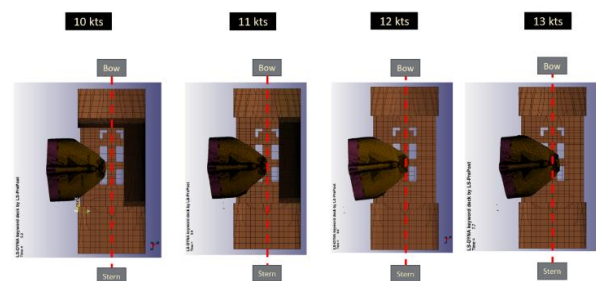


Figure 3 Collision Simulations to find the Relative Collision Speed

Collision Location: The middle of the vulnerable zone selected in STEP1 is determined as the

collision location. The RCOs will be applied on this target zone for damage stability improvement.

Collision Angle: A commonly recognised fact is that the highest internal energy materialises during a collision at a right-angle impact (Zheng et al., 2007, Hogstrom and Ringsberg, 2012), particularly when the impacted vessel is stationary. Therefore, to maintain a cautious and conservative stance, a collision angle of 90° is adopted.

Collision Draught and Trim: Differences in draught between the involved vessels can result in varying degrees of damage. Nonetheless, for the purposes of this paper, collisions are presumed to occur under even trim conditions at the designated design draught.

Step 3: Alternative Design Arrangements as RCOs

The third step involves the implementation of alternative design arrangements for (flooding) risk reduction, known as Risk Control Options (RCOs), to the target zones identified in the first step. These RCOs are not only intended to provide crashworthy arrangements, but also to reduce damage, especially transverse penetration, and increase buoyancy to improve the overall survivability of the ship. In order to assess the impact of RCOs on ship collisions, the crashworthiness analysis conducted in Step 2 with the use of RCOs should be repeated.

Step 4: Transverse Breach Distribution Update

After completing Step 3 and analysing the simulation results, the penetration reductions for each RCO arrangement can be determined. Using these reduced penetrations, the cumulative transverse breach distribution function of the target zone can be adjusted proportionally from a predetermined SOLAS CDF by shifting the point of 1 from the ship's centre (B/2) to the position of maximum penetration, as illustrated in Figure 12. This updated CDF can then be used to obtain the corresponding PDF for recalculating the damage stability.

Step 5: Damage Stability Re-evaluation

Once the new RCO arrangements and updated breach distribution have been established, the damage stability can be recalculated. This will enable the identification of the improvement in the Subdivision Attained Index resulting from each RCO.

Step 6: Cost-Benefit Analysis

The subsequent step involves conducting a cost-benefit analysis to determine the optimal RCO solution. In accordance with the FSA guidelines recommended by IMO (2018), the Gross Cost of Averting a Fatality (GCAF) is utilised to evaluate the cost-effectiveness of each RCO, as outlined below:

$$GCAF = \frac{\Delta Cost}{\Delta Risk} \quad (2)$$

The cost of each RCO encompasses both capital expenditure, such as material and labour costs, and operational costs, such as increased fuel consumption resulting from the added weight of RCO implementation. In terms of risk reduction, the reduction in expected fatalities (i.e., PLL) is utilised as a risk reduction factor. The EMSAIII (2013-2016) project risk models have been utilised for these calculations.

Step 9: Decision-Making

In the final step, the additional design, operation, maintenance aspects of the selected optimal RCOs must be thoroughly discussed and investigated by relevant decision-makers, including shipowners, shipbuilders, designers, class societies, and Administrations, to arrive at a final decision. Following this, an approval process may be initiated for the implementation of the selected RCOs in the construction or modification of the target ship.

3 CASE STUDY

To illustrate the application of this proposed methodology, a case study was undertaken using a reference cruise ship named FLOODSTAND SHIP B (Luhmann, 2009), simulating a collision scenario with a 45,000 GT RoPax vessel as the striking ship. The essential ship details are presented in Table 1.

Table 1 : Main Particulars of ships in the case study

	Target Ship	Striking Ship
LBP (m)	216.8	200.0
Breadth (m)	32.2	30.0
Displacement (tonne)	35,367	31,250
Pax Capacity	2,400	-

3.1 STEP 1: Vulnerability Analysis

The assessment of damage stability was conducted according to the prevailing SOLAS regulatory framework to ascertain the vulnerability of the original design for the reference vessel. The achieved Subdivision Index was calculated as 0.8579, falling short of the mandated Required Subdivision Index of 0.8676. This outcome indicates non-compliance with SOLAS regulations, as outlined in Table 2.

Table 2 : As-Built Design Damage Stability Results

Draught (m)	Trim (m)	GM (m)	Attained Index A	
Dl	6.890	0.120	2.670	0.1756
Dp	7.196	0.000	2.620	0.3429
Ds	7.400	0.000	2.720	0.3394
Attained Subdivision Index A			0.8579	
Required Subdivision Index R			0.8676	

Based on the outcomes of the damage stability analysis, the individual Attained Indices for each zone are compared to the maximum Index value. This maximum Index can be computed when the s-factor attains its highest value of 1 (i.e., the maximum local Subdivision Attained Index = $\sum p \times s_{max} = \sum p \times 1$). As highlighted within a black dashed rectangle in Figure 4, the zones between Z11 and Z18 exhibit lower local Indices for both the 3-zone and 4-zone damage scenarios. This signifies that the ship's survivability (s-factor) in case of damage occurring in these zones is relatively diminished, thereby classifying them as high-risk zones.

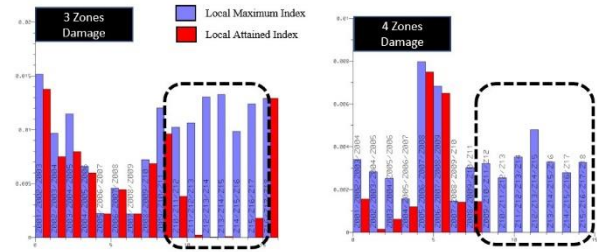


Figure 4 : Local Attained Index Loss

The quantification of these risks can be accomplished through the application of Equation (1), yielding the Index loss. However, a challenge arises in determining how much the Index loss of each zone contributes to the overall local Index loss in cases of multi-zone damage. To address this, the paper proposes a novel approach, an extension to adjacent zones, as a method for vulnerability analysis. This methodology assumes that the zone where the damage centre of each multi-damage case is located absorbs the entire Index loss, a concept sometimes referred to as a "winner-take-all" approach.

Furthermore, the adjacent zones' local Attained Indices also experience enhancement when the target zone exhibits heightened survivability. This implies that the risks of the adjacent zones are intertwined with the target zone. Consequently, the risk associated with the target zone is considered to result from the cumulative risk of three zones: the target zone itself and its two adjacent zones. Bae (2022) has substantiated this vulnerability analysis approach by comparing it to the individual enhancement outcomes of each zone under conditions of maximum survivability (i.e., zero permeability).

A comprehensive summary of the vulnerability analysis conducted on a reference vessel is presented in Figure 5.

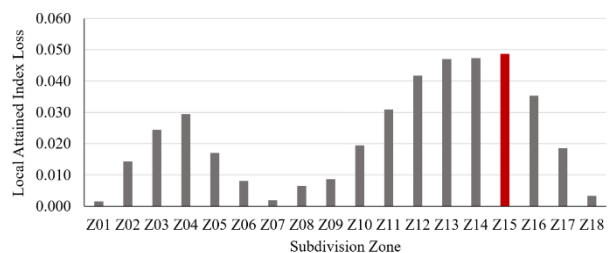


Figure 5: Local Risk of each Zone

3.2 STEP 2: Structural Crashworthiness Analysis

Subsequently, the collision simulations were executed utilising the ANSYS/LS-DYNA explicit code to address internal mechanics, complemented by the MCOL solver for external dynamics. A comprehensive breakdown of the specific parameters employed in these simulations, encompassing geometric modelling, material property characterisation, failure criteria, contact and friction considerations, as well as the delineation of hydrodynamic boundaries, is presented in the subsequent sections.

Geometry Modelling

The complete geometry of the reference ship was meticulously replicated, from zone 1 to zone 18. To achieve this, fine meshes serving as deformable regions were incorporated in the target zone 15 and its contiguous zones, namely Zone 14 and Zone 16. The remaining segments were configured with coarser meshes and identified as rigid components. Conversely, for the striking ship, solely the foremost 30.0 meters were considered for simulation, as this region is the only area undergoing deformation during collisions, as depicted in Figure 6. Furthermore, the Centre of Gravity (COG) and mass properties of the striking ship were factored into the MCOL solver, as elaborated in Table 3. In the simulation, the forepart of the striking ship was modeled using refined meshes and denoted as a deformable segment, while the end part was treated as rigid.

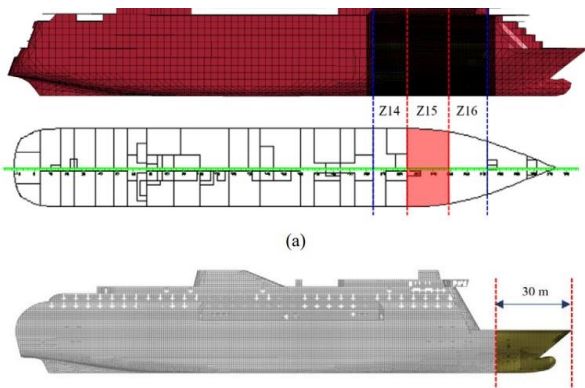


Figure 6: Geometric modellings with 2D shells

The fine meshes for the struck ship and the striking ship were designed with element sizes of

175 mm and 200 mm, respectively. These sizes were chosen as they are a quarter of the frame spacing for each respective ship, offering an economical yet reasonably accurate representation of the structural behaviour. Additionally, these mesh sizes adhere to the recommendation for fine meshing (i.e., less than 200 mm) as stipulated in AND 2009 guidelines.

For the simulation, Belytschko-Tsay 2D shell elements (LSTC, 2019) were employed. These elements incorporated a 5/6 shear factor and were integrated through the shell thickness with 5 integration points. This approach was implemented not only for the plate components but also for the stiffeners, ensuring a consistent modeling strategy across all geometries.

Material Property

Both vessels were considered to be constructed only from mild steel, and their material properties are outlined in Table 3. The collision simulations incorporated a Piecewise Linear Isotropic Plasticity material model (Hodge et al., 1956; LSTC, 2019). This model was applied to the contact areas constructed using fine meshes for both ships, enabling the observation of elastoplastic deformation resulting from collisions.

Table 3: Material properties for mild steel

Parameters	values
Density, ρ (kg/m ³)	7850
Young's modulus, E (MPa)	205,800
Poisson's ratio	0.3
Yield stress, σ_Y (Mpa)	235
Ultimate tensile strength (Mpa)	400

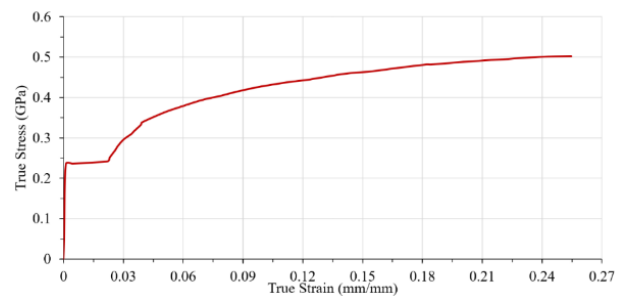


Figure 7 : Applied true stress/strain curve

In accordance with the given material properties, the simulation employed a true stress/strain curve as

described in Figure 7. This curve was extrapolated from experimental data (Paik, 2018) and was adjusted to be applicable within the simulation framework.

Failure Criteria and Dynamic Effects

The evaluation of structural response under impact loading is underpinned by the provided stress-strain curve established in the preceding section. However, a pivotal concern is the estimation of fracture points in finite element analysis. Over time, various authors have investigated and proposed a range of failure criteria. These encompass traditional constant failure strain criteria, criteria dependent on element size following Barba's law (Barba, 1880), strain-based failure criteria utilising forming limit diagrams, stress state-based failure criteria encompassing stress triaxiality, and criteria that account for crack propagation.

Given the complexity in selecting an optimal failure criterion, which can vary based on material properties, geometries, and collision scenarios, this paper adopts the through-thickness strain criterion introduced by Vredeveldt (2001) as expressed in Equation (3). This criterion, commonly known as the "GL criterion," is renowned for its simplicity and frequent application in FE analysis. It takes into consideration element size dependence and has been deemed the most widely employed failure criterion in FE analysis, endorsed by organizations such as IMO (2003) and UN (2008).

$$\varepsilon_c = \varepsilon_g + \varepsilon_e \frac{t}{l_e} \quad (3)$$

where, ε_c denotes critical fracture strain represented as $\varepsilon_{3f} = \varepsilon_c / (1 + \varepsilon_c)$, thinning strain ε_{3f} may be obtained from $\varepsilon_{3f} = -0.5(\varepsilon_1 + \varepsilon_2)$ based on the incompressibility condition with the Poisson ratio of 0.5. Uniform strain ε_g of 0.056 and necking strain ε_e of 0.540 were used for 2D shell element types (Scharer et al., 2002) used in these simulations.

In addition to the complexities of failure criteria, it's widely recognised that elevated strain rates can influence strain-stress curves by increasing dynamic yield stress. Strain rates are notably impacted by the initial collision energies, which in turn are contingent on variations in collision speeds.

Consequently, for collision simulations involving relatively high speeds, the consideration of strain rate effects becomes imperative. To address this concern, the formulation presented by Cowper and Symonds (1957) has been implemented. This formulation serves to account for the effects of strain rates and is structured as follows;

$$\frac{\sigma_{Yd}}{\sigma_Y} = 1.0 + \left(\frac{\dot{\varepsilon}}{C}\right)^{1/q} \quad (4)$$

Where σ_{Yd} and σ_Y are dynamic and static yield stresses, $\dot{\varepsilon}$ is strain rate, C and q are coefficients determined on the basis of test data. For mild steel, C=40.4 and q=5 have been used.

Contact and Friction Definition

Contact definition was established using the node-on-segment penalty method. For this purpose, the "Automatic Single Surface" option available in LS-DYNA was employed to set up contact in the finite element analysis. In terms of friction between colliding bodies, the friction coefficient has a notable impact on simulation outcomes. This is due to the separation of the initial collision energy into both frictional and internal energy components. Consequently, a significant increase in friction energy can lead to a reduction in internal energy, and vice versa. Given these considerations, the selection of the friction coefficient demands careful attention. Engineering references suggest a range of 0.09 to 0.19 for lubricated mild steel surfaces and a coefficient of 0.57 for non-lubricated surfaces. In practice, industry standards and several works in the literature, including Sajdak and Brown (2005) and Paik (2007), advise adopting dynamic friction coefficients within the range of 0.1 to 0.3 for the sake of simplification.

Considering the typical conditions of vessel hull, which are often affected by biofouling, a value of 0.3 for the dynamic friction coefficient was thought to be a reasonable choice

Hydrodynamic Boundary Definition

Historically, numerous collision simulations have often limited the translational degrees of freedom. Nonetheless, the accurate representation of hydrodynamic boundary conditions in ship

collisions is pivotal, as it encompasses the external dynamics of both vessels. This includes factors like the restoring forces linked to ship mass and buoyancy, the added mass of both ships, and the damping forces induced by wave actions.

In this study, the MCOL solver, integrated within LS-DYNA, was harnessed to account for these intricate ship motions and added mass effects in the finite element analysis. The input parameters for this solver were computed using ANSYS AQWA (ANSYS, 2019), leveraging the ship characteristics detailed in Table 4. This approach enabled a comprehensive consideration of the complex hydrodynamic interactions in collision scenarios.

Table 4: Hydrodynamic input for ship motions

Parameters	Struck ship	Striking ship
Draft (m)	7.2	6.9
Displacement (tonne)	35,367	31,250
LCG (m)	99.29	85
KG (m)	15	14
Gyration radius (m)	Surge 10.95	11
	Sway 54.20	55
	Heave 56.37	55

Collision Scenario Definition

This phase involves the specification of a collision scenario that will be utilised in the finite element analysis. Six key parameters have been primarily considered for this purpose, including the striking ship, collision speed, collision location, collision angle, draft, and trim.

In this context, the 45,000 GT RoPax has already been assigned as the striking ship. As a result, the geometric configuration of its bow shape and the ship mass have been ascertained from the provided striking ship drawings and its main particulars, respectively. Zone 15 has been identified as the most vulnerable region of the reference vessel, as determined in STEP 1. The collision angle is set at 90° and the trim is assumed to be at the design draft. Given these considerations, the only remaining parameter is the collision speed, which will be the focal point of this scenario definition.

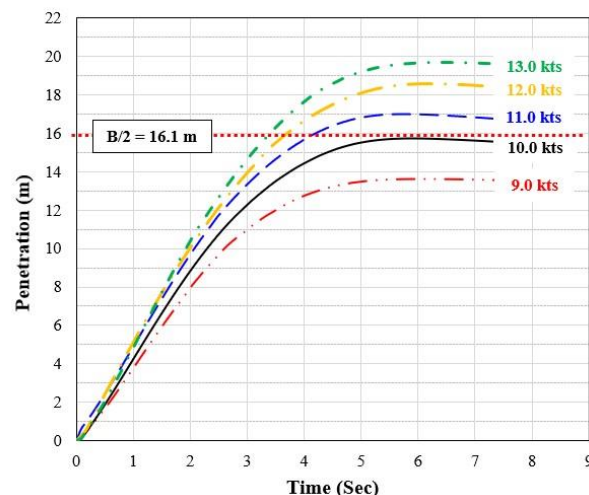


Figure 8 : Collision Simulations Results

To determine the relative speed that results in the maximum penetration of B/2, a sequence of simulations has been executed. It is important to emphasise that the simulation configuration used for the finite element analyses should also be maintained for these preliminary simulations. Figure 8 shows the variation in maximum penetration over time across different speeds. Notably, a collision speed of 10.14 knots yields transverse penetration closest to B/2. With this insight, the collision scenario for the simulations involving the reference ship and the striking ship can be succinctly summarised in Table 5.

Table 5 : Summary of Collision Scenario

Ships	speed (knots)	angle (°)	From A.P. (m)	Draft (m)
Struck ship	0	0	0	7.2
Striking ship	10.14	90	165.8(*)	6.9

3.3 STEP 3: Risk Control Option Applications

To manage and mitigate damage stability risks, alternative design arrangements in the form of RCOs have been implemented. The RCOs considered in this case study are comprehensively outlined in Table 6. A total of 6 RCOs were thoroughly examined, falling under the categories of passive measures. These measures can be categorized into two distinct types: those involving a single longitudinal bulkhead at varying locations and measures that entail reinforcing the hull thickness.

Table 6 : Applied Risk Control Options

Name	Description
RCO1	Single LBHD at B/20
RCO2	Single LBHD at 2B/20
RCO3	Single LBHD at 3B/20
RCO4	Single LBHD at 4B/20
RCO5	20T hull + Single LBHD at 10.6m (*)
RCO6	30T hull + Single LBHD at 6.6m (*)

(*) Locations to be out of the maximum penetrations

This type of passive measure is referred to as the "double-hull concept," a concept already implemented in tankers and LNG carriers to mitigate environmental risks such as oil spills or gas leaks resulting from ship collisions. The single longitudinal bulkhead on each side is assumed to be installed from a double bottom on deck 1 to the embarkation deck on deck 5, as illustrated in Figure 9. These bulkheads are constructed using mild steel with a thickness of 10mm. Two wing compartments on each side, formed by each longitudinal subdivision, are connected to one another through cross-flooding arrangements.

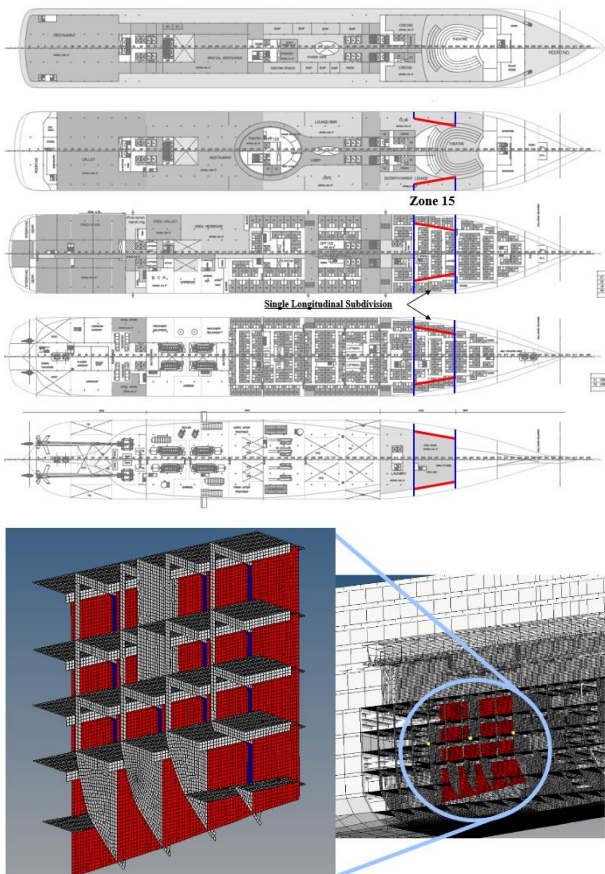


Figure 9 : Single LBHD Arrangements

Specifically, the RCOs were explored with four distinct plate installation positions: B/20, 2B/20, 3B/20, and 4B/20. Here, B/20 pertains to the criterion for the double bottom height. Additionally, B/10 serves as the position criterion not only for the maximum penetration as defined in the current SOLAS Reg.II-1/B-1/8 but also as one of the recommendations for maximum transverse penetration during the establishment of SRtP regulations. Furthermore, B/5 aligns with the criteria for maximum damage penetration for RoPax vessels in accordance with the Stockholm Agreement (EU, 2003). For tankers with fuel oil capacities exceeding 5,000m³, MARPOL regulations (IMO, 2004) stipulate requirements for a distance between the longitudinal bulkhead and the hull, ranging from 1.0m to 2.0m depending on the fuel oil capacity.

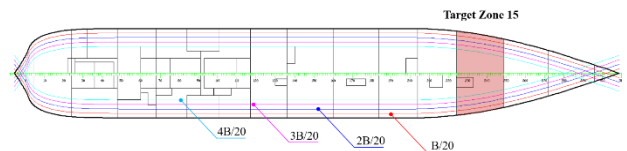


Figure 10 : Different Locations of LBHD

FE analysis results

Based on the established simulation configuration and the defined collision scenario, a series of simulations were conducted for each RCO, utilizing a collision speed of 10.14 m/s. Figure 11 provides an overview of the penetration results obtained from finite element analysis (FEA) for each RCO.

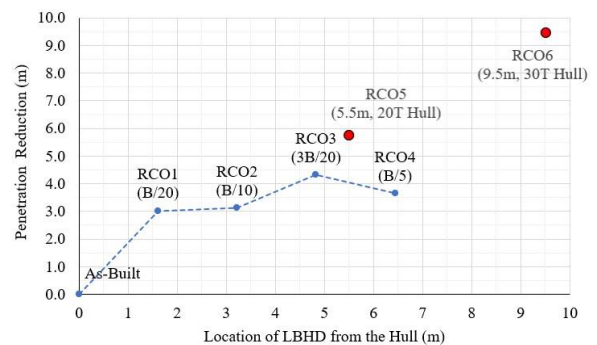


Figure 11 : Penetration Reductions for each RCO

For RCO1, RCO2, RCO3, and RCO4, transverse penetrations ranged from 3.3m to 4.3m depending on the Longitudinal Bulkhead Distance (LBHD) locations. Notably, these RCOs revealed a reduction in transverse penetrations, with the LBHD

effectively absorbing collision energy and contributing to a decrease in transverse penetration by approximately 3.5m. However, it's important to note that the specific location of each different RCO had a minimal impact on the penetration reduction.

In contrast, RCO5 and RCO6, which involve the reinforcement of the hull to 20T and 30T thickness, respectively, demonstrated more substantial improvements. These two measures led to explicit penetration reductions of 5.7m and 9.6m, highlighting their effectiveness in enhancing collision resistance.

3.4 STEP 4: Transverse Distribution Update

Utilizing the results from the finite element analysis conducted in STEP 3, adjustments can be made to the local transverse distribution associated with zone 15. The cumulative distribution function (CDF) can be updated by proportionally accounting for the reduction in penetration. This adjustment involves shifting the point of maximum penetration from the initial value of 16.1m (B/2) to the calculated actual transverse penetration measured from the hull of the struck ship.

Figure 12 visually illustrates the updated probability density function (PDF) and CDF for RCO6 in comparison to the original distribution stipulated in the current SOLAS regulation for the p-factor. Subsequently, the updated PDF can be deduced from the adjusted CDF. The new PDF, represented by the red column, can then replace the original PDF shown in the blue column (i.e., the old p-factor). As a consequence, the updated p-factor for damage cases will undergo an increase, achieved by multiplying it with the s-factors. This, in turn, leads to improvements in the local Attained Indices.

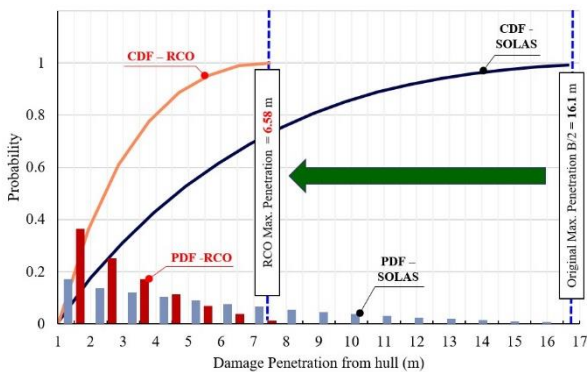


Figure 12 : Suggested Methodology for Transverse Distribution (p-factor) Update

If the RCO arrangement results in increased s-factors, then the enhancement in the Attained Index will be more pronounced, providing a substantial enhancement in damage stability performance.

3.5 STEP 5: Damage Stability Re-evaluation

Having integrated the RCO arrangement and adjusted local transverse breach distribution (p-factor) within the target zone 15, a comprehensive reassessment of the reference ship's damage stability was undertaken. This re-evaluation was conducted in adherence to the prevailing SOLAS regulations, with the primary objective of identifying the collective enhancement in the Attained Index, which serves as a measure of improved damage stability.

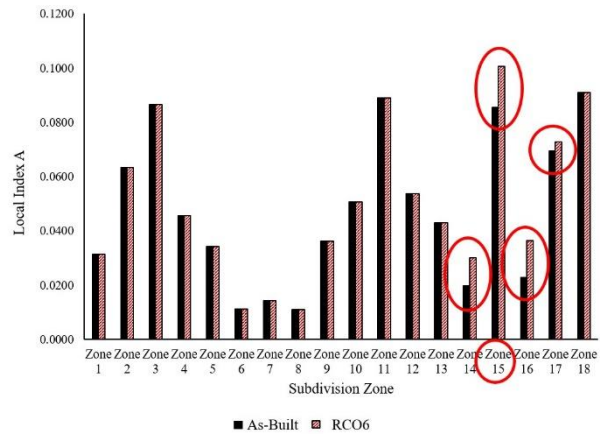


Figure 13 : RCO6 -Local Attained Index Improvement

With the updated breach distribution in Zone 15, the local p-factors within the range of transverse penetration have undergone changes. The new p-factors for damage cases within the transverse penetration zone have increased, attributed to the augmentation of the probability density function (PDF) in that range, as illustrated by the red column in Figure 12. However, the old p-factors between 6.58m and 16.1m (depicted by the blue column) have become irrelevant for calculation purposes since this region is free from damages (refer to Figure 12). Regarding s-factors in Zone 15, the local s-factors have experienced improvement through the application of the RCO arrangement. Consequently, the local Attained Indices (sum of p-factor × s-factor) of not only Zone 15 but also Zones 14, 16, and 17 have been elevated, as described in Figure 13. Interestingly, the impact of the RCOs extends beyond the target zone and influences adjacent

zones, introducing relevant risks to those zones as well, which is instrumental for the vulnerability analysis conducted in STEP 1. Especially, for RCO6, the overall Attained Index has been heightened by 3.46%, ascending from the original value of 0.8579 to 0.8925. The outcomes of the damage stability re-assessment for the other RCOs are succinctly presented in Table 7.

Table 7 : Summary of Damage Stability Recalculation for all RCOs

RCO	Attained Index	Increase (%)
As-Built	0.8579	-
RCO1	0.8590	+ 0.11
RCO2	0.8619	+ 0.41
RCO3	0.8692	+ 1.13
RCO4	0.8727	+ 1.48
RCO5	0.8816	+ 2.38
RCO6	0.8925	+ 3.46

3.6 STEP 6: Cost-Benefit Analysis

The final step involves the selection of an optimal solution or solutions among the RCOs, taking into account the costs associated with each RCO. This is accomplished through cost-benefit analysis employing the Gross Cost of Averting a Fatality (GCAF), defined as $GCAF = \Delta Cost / \Delta Risk$. To estimate the costs of each RCO, the unit costs outlined in the EMSA III project have been adopted as followings;

- 6,600 USD/ton : Steel weight, including piping, ducting, painting
- 3,300 USD/m² : Public areas, including ducting, cabling etc
- 2,750 USD/ m² : Cabin and Service areas, including ducting, cabling
- 33,000 USD/pcs : Additional Watertight Sliding Door, including cabling (*)
- 275 USD/m² : Cost for penetration watertight subdivision including ducting and cabling etc.(*)
- 418 USD/kW : Additional installed power of main engines, taking into account any discrete step in engine size

(*)An additional 20% of the door cost is included for penetrations of ducting and cabling on the subdivision.

These unit costs are considered based on an exchange rate of 1.1 between Euro and USD in 2015. Additionally, the increased fuel costs due to the additional weights of each RCO are evaluated. These increases are calculated using data from NAPA, and the assumption is made that the increase in wetted area directly impacts ship fuel consumption. This is because friction resistance, which constitutes a significant portion of total ship resistance, is influenced by the wetted surface area. The costs of various types of fuel, including 60% Heavy Fuel Oil (HFO), 20% Marine Gas Oil (MGO), and 20% low sulfur HFO, are presumed to be 600 USD/ton, 900 USD/ton, and 840 USD/ton, respectively, based on EMSA (2015) data.

The expected reduction of fatalities (ΔPLL) was defined as risk reduction ($\Delta risk$) and the same assumption in EMSAIII (2013-2016) was adopted for Potential Loss of Life (PLL) calculations:

$$PLL_{total} = PLL_{collision} + PLL_{grounding/contact} + PLL_{fire/explosion} \quad (5)$$

The risk models for both collisions and groundings, as defined in the EMSA III project, have been utilized for this analysis. However, there has been an update to the sinking probability in these modes. This update is based on the update final Attained Index calculated for each RCO in STEP 5, reflecting the enhanced damage stability achieved through the RCO arrangements.

The necessary cost and the corresponding PLL for each RCO are concisely summarized as following Table.

Table 8 : Cost and PPL Calculated for each RCO

RCO	Cost (Mil USD)	PPL	Δ PPL
As-Built	-	4.64	-
RCO1	0.55	4.59	- 0.05
RCO2	0.58	4.44	- 0.20
RCO3	0.62	4.09	- 0.55
RCO4	0.64	3.92	- 0.72
RCO5	1.22	3.48	- 1.16
RCO6	1.94	2.95	- 1.69

3.7 STEP 7: Decision Making

The outcomes of the cost-benefit analysis are visually summarized in Figure 14, which presents the Gross Cost Assessment Factor (GCAF) values corresponding to the improved Attained Index for all 6 RCOs applied to the reference ship. These GCAFs are derived from the detailed results obtained at each step of the analysis:

- Penetration reductions from Figure 11
- Attained Index improvements from Table 6
- RCO costs from Table 7
- Risk reduction (Δ PPL) from Table 7

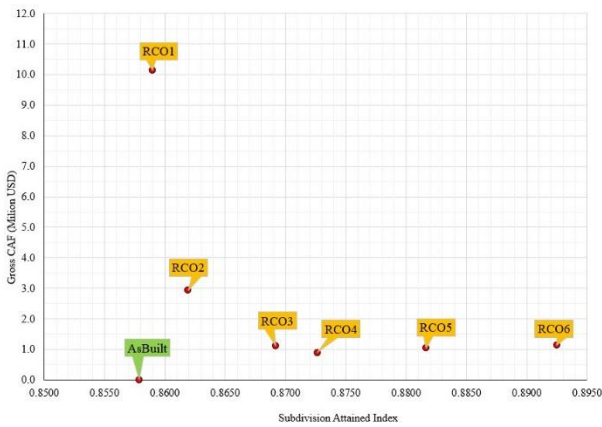


Figure 14: Summary of Cost Benefits Analysis

Based on the graph, it's evident that RCO6, characterized by a hull thickness of 30T and a single longitudinal bulkhead positioned 6.6m from the ship's centerline, emerged as the most effective measure. It obtained a GCAF of 1.09, thereby offering the highest survivability with an Attained Index of 0.8925. It's worth noting, however, that the placement of the single longitudinal bulkhead in RCO6 is relatively close to the ship's centerline compared to the other risk control options. This implies that the inner spaces confined by the two bulkheads might be constrained, potentially leading to reduced flexibility in terms of space utilization.

Given these considerations, the final decision-making process for the optimum solution should carefully weigh the advantages and disadvantages of RCO6. This entails a comprehensive evaluation of its potential benefits and drawbacks within the context of the ship's design and intended purpose.

4 CONCLUSIONS / RECOMMENDATIONS

This paper introduces a novel methodology for enhancing ship survivability through crashworthiness analysis, focusing on alternative designs not covered by the current SOLAS framework. The methodology, consisting of seven distinct steps, has been demonstrated using a 65,000 GT cruise ship as a case study. Within this context, six Risk Control Options (RCOs) were considered to either control or mitigate risks.

The process began with a vulnerability analysis utilizing a plurality approach with extension to adjacent zones. This analysis identified Zone 15 as the target zone and collision location. Subsequently, the collision scenario, involving a collision speed of 10.14 knots to yield maximum B/2 penetration, was defined. Collision simulations for each RCO followed, leading to the acquisition of penetration reduction results. The local transverse breach distribution of the target zone was updated for each RCO, enabling the re-assessment of damage stability and the computation of improved Attained Indices. cost-benefit analyses encompassing both CAPEX and OPEX for a ship's 30-year life cycle were conducted. This entailed calculating Potential Loss of Life (PLL) reduction for each RCO, using risk models from the EMSA III project and the results of damage stability re-assessment.

The culmination of the analysis is to quantify effects of each RCOs using crashworthiness analysis, using penetration and attained index. Then, in turn, the design effects of each RCO were plotted with the GCAF and Attained Index, to identify the optimal solution among RCOs. The selected optimum RCO involves a double hull design with a single longitudinal subdivision positioned at 6.6m and strengthened hull thickness of 30mm. However, while RCO6 proves advantageous in terms of cost and risk reduction, associated limitations related to design, operation, and maintenance should be meticulously assessed by decision-makers prior to final implementation.

Based on this proposed quantitative risk assessment methodology and analysis outcomes, it is recommended that the implementation of RCOs across adjacent zones and the target zone can lead to more versatile and spacious internal spaces. This potential innovation could pave the way for

significant design advancements in the future, fostering a new paradigm for ship design.

5 REFERENCES

- ANSYS 2019. User's manual for ANSYS AQWA version 18. In: INC., A. (ed.). PA, USA.
- BAE, H., VASSALOS, D., PATERSON, D., MUJEEB-AHMED, M. & BOULOUGOURIS, E. 2021. The Effectiveness of Crashworthiness as a Damage Stability Risk Control Option. Conference: 1st International Conference on the Stability and Safety of Ships and Ocean Vehicles (STAB&S 2021). Glasgow, UK
- BARBA, M. 1880. Mémoires de la Société des Ingénieurs Civils. *Memoirs of the Society of Civil Engineers*, 22.
- COWPER, G. R. & SYMONDS, P. S. 1957. Strain-hardening and strain-rate effects in the impact loading of cantilever beams. Brown Univ Providence Ri.
- EHLERS, S., BROEKHUIJSEN, J., ALSOS, H. S., BIEHL, F. & TABRI, K. 2008. Simulating the collision response of ship side structures: a failure criteria benchmark study. *International Shipbuilding Progress*, 55, 127-144.
- EMSA 2015. Risk Acceptance Criteria and Risk Based Damage Stability, Final Report, Part 2: Formal Safety Assessment.
- EMSIII 2013-2016. Study assessing the acceptable and practicable risk level of passenger ships related to damage stability ("EMSA 3"), undertaken by DNVGL. EMSA/OP/10/2013, <http://emsa.europa.eu/damage-stability-study.html>.
- EU 2003. THE EUROPEAN PARLIAMENT AND OF THE COUNCIL of 14 April 2003 on specific stability requirements for ro-ro passenger ships. *DIRECTIVE 2003/25/EC*. Official Journal of the European Union.
- HARDER 2000-2003. Harmonisation of Rules and Design Rationale. EC Contact No. GDRB-CT-1998-00028, Final Technical Report.
- HODGE, P., HOPKINS, H. & LEE, E. 1956. The theory of piecewise linear isotropic plasticity. *Deformation and Flow of Solids/Verformung und Fließen des Festkörpers*. Springer.
- HOGSTRÖM, P. & RINGSBERG, J. W. 2012. An extensive study of a ship's survivability after collision—a parameter study of material characteristics, non-linear FEA and damage stability analyses. *Marine structures*, 27, 1-28.
- IMO 1991. Explanatory notes to the SOLAS regulation on subdivision and damage stability of Cargo ships of 100 meters in length and over. Res.A.684(17). the Assembly, International Maritime Organisation, London, UK.
- IMO 2003. DEVELOPMENT OF EXPLANATORY NOTES FOR HARMONIZED SOLAS CHAPTER II-1, Approval procedure concept for alternative arrangements, Submitted by Germany. SLF 46/INF.10. SUB-COMMITTEE ON STABILITY AND LOAD LINES AND ON FISHING VESSELS SAFETY, International Maritime Organisation, London, UK.
- IMO 2004. Amendments to the Annex of the Protocol of 1978 relating to the International Convention for the Prevention of Pollution From Ships, 1973. Res.MEPC.117(52) Reg.19 & 20. Marine Environment Protection Committee, International Maritime Organisation, London, UK.
- KIM, S. J., KORGERSAAR, M., AHMADI, N., TAIMURI, G., KUJALA, P. & HIRDARIS, S. 2021. The influence of fluid structure interaction modelling on the dynamic response of ships subject to collision and grounding. *Marine Structures*, 75, 102875.
- LSTC 2019. LS-DYNA keyword user's manual. In: CORPORATION, L. S. T. (ed.). California, USA.
- LUHMANN, H. 2009. Floodstand WP1 Deliverable D: Concept ship desing B.
- PAIK, J. 2007. Practical techniques for finite element modeling to simulate structural crashworthiness in ship collisions and grounding (Part I: Theory). *Ships and Offshore Structures*, 2, 69-80.

- PAIK, J. K. 2018. Ultimate limit state analysis and design of plated structures, Wiley Online Library.
- PAIK, J. K., KIM, S. J., KO, Y. K. & YOUSSEF, S. A. Collision risk assessment of a VLCC class tanker. SNAME Maritime Convention, 23-28 October 2017 2017 Houston, USA. The Society of Naval Architects and Marine Engineers.
- PATERSON, D. 2020. Reconfiguring the ship environment for damage stability enhancement. University of Strathclyde.
- SAJDAK, J. & BROWN, A. 2005. Modeling longitudinal damage in ship collisions. SSC-437, Ship Structure Committee.
- SCHARRER, M., ZHANG, L. & EGGE, E. 2002. Kollisionsberechnungen in schiffbaulichen entwurfssystemen (collision calculation in naval design systems). Bericht ESS 2002.183. Germanischer Lloyd.
- SCHREUDER, M., HOGSTRÖM, P., RINGSBERG, J. W., JOHNSON, E. & JANSON, C. E. 2011. A method for assessment of the survival time of a ship damaged by collision. Journal of ship research, 55, 86-99.
- UN 2008. European Agreement concerning the international Carriage of Dangerous Goods by Inland Waterways (ADN). ECE/TRANS/203 (Vol.I). United Nations, New York and Geneva.
- VASSALOS, D., MUJEEB-AHMED, M., PATERSON, D., MAURO, F. & CONTI, F. 2022. Probabilistic damage stability for passenger ships—the p-factor illusion and reality. Journal of Marine Science and Engineering, 10, 348.
- VREDEVELDT, A., FEENSTRA E 2001. Crashworthy side structures for improved collision damage survivability of coasters and medium sized Ro-Ro cargo ships.
- ZHANG, L., EGGE, E.-D. & BRUHNS, H. 2004. Approval procedure concept for alternative arrangements, Germanischer Lloyd.
- ZHENG, Y., AKSU, S., VASSALOS, D. & TUZCU, C. 2007. Study on side structure resistance to ship-ship collisions. Ships and Offshore Structures, 2, 273-293.